

ORIGINAL ARTICLE

Two nonsense *GLI3* variants are associated with polydactyly and syndactyly in two families by affecting the sonic hedgehog signaling pathway

Xiaofang Shen^{1,2} | Shun Zhang^{3,4} | Xin Zhang⁵ | Taifeng Zhou^{3,4} | Yongjun Rui⁶ ¹Soochow University, Suzhou, China²Department of Orthopedics, Children's Hospital of Soochow University, Suzhou, China³Department of Orthopedics, First Affiliated Hospital, Sun Yat-sen University, Guangzhou, China⁴Guangdong Provincial Key Laboratory of Orthopedics and Traumatology, First Affiliated Hospital, Sun Yat-Sen University, Guangzhou, China⁵Department of Clinical Research Unit, Tongji Hospital, Tongji University School of Medicine, Shanghai, China⁶Department of Orthopedics, Wuxi Ninth People's Hospital Affiliated to Soochow University, Wuxi, China**Correspondence**

Yongjun Rui, Department of Orthopedics, Wuxi Ninth People's Hospital Affiliated to Soochow University, 999 Liangxi Road, Wuxi, Jiangsu 214062, China.
Email: ruiyj@hotmail.com

Taifeng Zhou, The Department of Orthopedics, the First Affiliated Hospital, Sun Yat-sen University, 58 Zhongshan Second Road, Guangzhou, Guangdong 510080, China.
Email: zhoutaif@mail2.sysu.edu.cn

Funding information

This work was supported by the National Natural Science Foundation of China (Nos. 92068105; 82072385; and 81772293).

Abstract

Background: Polydactyly and syndactyly are congenital limb deformities, segregating in an autosomal-dominant fashion. The variants in the *GLI3* gene are closely related to congenital limb malformations. However, the causes underlying polydactyly and syndactyly are not well understood.

Methods: We conducted a whole-exome sequencing on two four-generation Chinese families with polydactyly and syndactyly. Then c.2374C>T and c.1728C>A mutant plasmids were transfected to HEK293T cells and mice limb bud cells to explore the functional consequences of these variants. Western blot and real-time quantitative PCR were used to analyze the expression of *GLI3* and *Shh*.

Results: In these two families, the known *GLI3* variant (NM_000168.6:c.2374C>T) and the novel *GLI3* variant (NM_000168.6:c.1728C>A) contributed to polydactyly and syndactyly. Additionally, the *GLI3* c.2374C>T mutant plasmid led to truncated *GLI3* protein, and the *GLI3* c.1728C>A mutant plasmid led to degraded *GLI3* protein. Simultaneously, we demonstrated that the *GLI3*-mutant plasmids led to decreased *Shh* expression in mice limb bud cells.

Conclusion: We demonstrated that the novel *GLI3* variant (c.1728C>A) and known *GLI3* variant (c.2374C>T) contributed to the malformations in two four-generation pedigrees with polydactyly and syndactyly by affecting SHH signaling.

Xiaofang Shen and Shun Zhang contributed equally to this work.

This is an open access article under the terms of the Creative Commons Attribution-NonCommercial-NoDerivs License, which permits use and distribution in any medium, provided the original work is properly cited, the use is non-commercial and no modifications or adaptations are made.

© 2022 The Authors. *Molecular Genetics & Genomic Medicine* published by Wiley Periodicals LLC.

KEYWORDS

GLI3, polydactyly, syndactyly, variant, whole-exome sequencing

1 | INTRODUCTION

Polydactyly is the most frequently observed congenital hand malformation, with a prevalence of approximately two per 1000 live births (Anderson et al., 2012). Syndactyly is characterized by a cutaneous or osseous fusion of adjacent digits, which is one of the most common forms of all congenital hand deformities with an incidence of around 1 in 2000 live birth (Jordan et al., 2012). Polydactyly and syndactyly both segregate in an autosomal-dominant fashion.

Human limb bud development is a highly complex and conserved pattern, which is the basis of digits development (Petit et al., 2017). Sonic hedgehog (SHH) signaling pathway acts an important role to regulate the digits pattern in limb formation, specifying anteroposterior pattern in developing limbs. And glioma-associated oncogene homolog 3 (*GLI3*, OMIM: 165240), a zinc finger transcription factor, is one of the most important downstream factors in the SHH signaling pathway (Al-Qattan et al., 2017; Villavicencio et al., 2000). *GLI3* has two kinds of forms, full-length (*GLI3*-FL) and repressor (*GLI3*-R) form. When the SHH signaling pathway is absent, *GLI3* is phosphorylated and partially degraded or converted to *GLI3*-R which leads to repression of the SHH signaling pathway. When the SHH signaling is present, *GLI3*-FL specifically targets the promoter of *GLI1* to regulate SHH signaling pathway-associated genes (Matissek & Elswa, 2020).

The role of *GLI3* in limb development is widely studied in two kinds of human congenital malformations including Pallister–Hall syndrome (PHS) and Greig cephalopolysyndactyly syndrome (GCPS). Pallister–Hall syndrome is a pleiotropic autosomal-dominant disorder comprising visceral malformations, pituitary dysfunction, central polydactyly, and hypothalamic hamartoma (Hall, 2014). Johnston et al. (2005) reported that *GLI3* mutations that predicted a truncated functional repressor protein caused Pallister–Hall syndrome. Greig cephalopolysyndactyly syndrome is characterized by preaxial and postaxial polydactyly, variable syndactyly, scaphocephaly, frontal bossing, and hypertelorism (Biesecker, 2008). Using a candidate gene approach to test the possible implication of the *GLI3* gene in this disorder, Vortkamp et al. (1991) demonstrated that two of three translocations were associated with GCPS by interrupting the *GLI3* gene. These studies demonstrate that the variants in the *GLI3* gene are closely related to congenital digit malformations.

In this study, we explored the genetic basis of polydactyly and syndactyly in two four-generation Chinese families. Using whole-exome sequencing followed by Sanger sequencing, we identified a novel heterozygous nonsense variant c.1728C>A (p.Y576X) in *GLI3* that segregated with the disease phenotype within Family 2. We also identified a known nonsense variant c.2374C>T (p.R792X) using whole-exome sequencing in Family 1, and this point variant was previously reported to be associated with polydactyly and syndactyly (Furniss et al., 2007). In vitro, we observed that these two variants led to truncated or degraded *GLI3* protein. Meanwhile, the *Shh* expression levels were decreased when mice limb bud cells were transfected with mutant plasmids, which resulted in limb malformations.

2 | MATERIALS AND METHODS

2.1 | Subjects

Two four-generation Han Chinese pedigrees with polydactyly and syndactyly were identified. In Family 1, 17 family members (6 affected members and 11 normal members) participated in this study. In Family 2, 34 family members (11 affected members and 23 normal members) participated in this study. Polydactyly and syndactyly were diagnosed based on X-ray examination, physical examination, and family history. DNA samples were extracted from peripheral blood using QIAamp DNA blood mini kits (Qiagen, Germany).

2.2 | Genetic studies

Exome sequences were enriched with an Agilent SureSelect Human All Exon V6 Kit (Agilent Technologies, Santa Clara, CA). Sequences were generated on a HiSeq PE150 (Illumina). Base-calling was performed, and raw-sequencing read files were generated in FASTQ format. Subsequently, we aligned the sequenced reads to the reference human genome (NCBI Build 37, hg19) and performed the annotation using SeattleSeq Annotation 150 (version 9.10). In this study, the GenBank reference sequence and version number is NC_000007.13.

We then used various databases to predict and filter all variants, such as the database of single nucleotide polymorphisms (dbSNP), 1000 genomes, SIFT, Polyphen-2, and Mutation Taster. All variants included in the most recent version of the National Center for Biotechnology Information

dbSNP were excluded. Low-frequency frameshift and truncating variants (minor allele frequency <0.001) in any genes were considered potentially pathogenic. Finally, we chose variants that were shared by affected individuals but not present in the unaffected individual.

2.3 | Genotyping

Genomic DNA was isolated from 200 μ l of blood per subject and was diluted to a final concentration of 15–30 ng/ μ l for genotyping assays. Polymorphism-spanning fragments were amplified using PCR and genotyped using the MassArray system (Sequenom, San Diego, CA) with primers of c.17280C>A (Fwd: TGACCAGTAGGTGGCAGTT, Rev: GCTACATCTGAATCCCAATAAA), prepared by the Beijing Genomics Institute (Shenzhen, China), as described previously (Gao et al., 2017).

2.4 | Plasmid constructs and transfection

Full-length, wild-type (WT) human *GLI3* cDNA was amplified (Fwd: 5'-CGCAAATGGGCGGTA GCGTG-3', Rev: 5'-TAGAAGGCACAGTCGAGG-3'), and *GLI3* cDNA was cloned into H302 pcDNA3.1(+) vector (Obio corporation, Shanghai, China). Mutagenesis of *GLI3* (to introduce variants encoding the p.R792X and p.Y576X) was performed using a QuikChange Lightning Site-Directed Mutagenesis kit (Stratagene, Santa Clara, California). HEK293T cells and mice primary limb bud cells were seeded in six-well plates and transiently transfected with plasmids using Lipofectamine 3000 (Invitrogen). Cells were harvested 48 hr after transfection.

2.5 | Cells culture

Primary mice limb buds are isolated from embryonic day 11.5 under a stereo light microscope and digested with 0.25% trypsin for 10 min at 37 °C. Limb bud cells were seeded in a six-well plate and cultured at 37 °C with 5% CO₂. DMEM (Gibco) supplemented with 1% penicillin–streptomycin solution (Gibco), and 10% fetal bovine serum (PAN) was used as the culture medium. HEK293T cells were cultured in DMEM (Gibco) high glucose containing 10% fetal bovine serum (Gibco) at 37 °C with 5% CO₂.

2.6 | Western blot analysis

The proteins of HEK293T cells were extracted with RIPA buffer (Beyotime) containing 1% phosphatase

and protease inhibitors (Bimake), followed by measurement of protein concentrations using a BCA protein assay (Beyotime). After boiling denaturation, the protein samples (20 μ g/sample) were subjected to 7.5% SDS-PAGE and then transferred to nitrocellulose membranes (Pall). After being blocked with 5% skim milk for 1 hr at room temperature, the membranes were probed with primary antibody against Flag (101274-MM05, Sino Biological), HA (100028-MM10, Sino Biological) at 4 °C overnight and then washed three times with TBS-T before incubation with antimouse secondary antibody (7076, Cell Signaling Technology) for 1 hr at room temperature. Color development was performed using an ECL chemiluminescence detection kit (Beyotime, Shanghai, China), and images of protein bands were captured using a gel imager (GE, ImageQuant Las4000mini).

2.7 | Real-time quantitative PCR

Total RNA was extracted from mouse limb bud cells with RNAiso Plus reagent (Roche). cDNA was synthesized using 500 ng of total RNA and a Prime-Script RT reagent kit with a gDNA Eraser (Takara) following the manufacturer's instructions. Quantitative PCR was performed to amplify the cDNA on a Bio-Rad CFX96 Real-Time PCR System using TB Green Premix Taq II (Takara, Japan) and primers (Fwd: AAAGCTGACCCCTTTAGCCTA; Rev: TTCGAGTTTCTTG TGATCTTCC). Relative expression levels were calculated by the $2^{-\Delta\Delta Ct}$ method. GA0PDH served as the internal control for normalization.

2.8 | Statistical analysis

Statistical analysis was performed using the statistical software SPSS13. Results are expressed as mean \pm standard deviation (s.d.) and analyzed for significant differences using analysis of variance (ANOVA) and Student's *t* test. $p < .05$ was considered significant (* $p < .05$, ** $p < .01$, *** $p < .001$).

3 | RESULTS

3.1 | Clinical assessment of two families with polydactyly and syndactyly

Two four-generation families with polydactyly and syndactyly from Wuxi Ninth People's Hospital Affiliated to Soochow University were recruited for the study. No history of consanguineous marriage in this family was

recorded according to the senior family members' statements. In these two families, the family history of the disorders was consistent with an autosomal-dominant pattern of inheritance. Phenotypic variability was observed among affected individuals.

The clinical assessment of five affected members in Family 1 was summarized in Figure 1 and Table 1. The clinical assessment of six affected members in Family 2 was summarized in Figure 2 and Table 2. The depth and coverage of whole-exome sequencing in Family 2 were presented in Table 3. According to the clinical assessment

of these two families, we observed phenotypic variability among affected individuals which was consistent with previous research. Except for polydactyly and syndactyly, there were no other abnormalities of the shape of the head, maxillofacial malformation, brain imaging, distance of the inner canthal, interpupillary distance, height or limb length, organa genitalia, anus, and throat (epiglottis) observed in these two families. All the patients in Family 1 were diagnosed as synpolydactyly-1 (OMIM: 186000), all the patients in Family 2 were diagnosed as synpolydactyly-3 (OMIM: 610234).

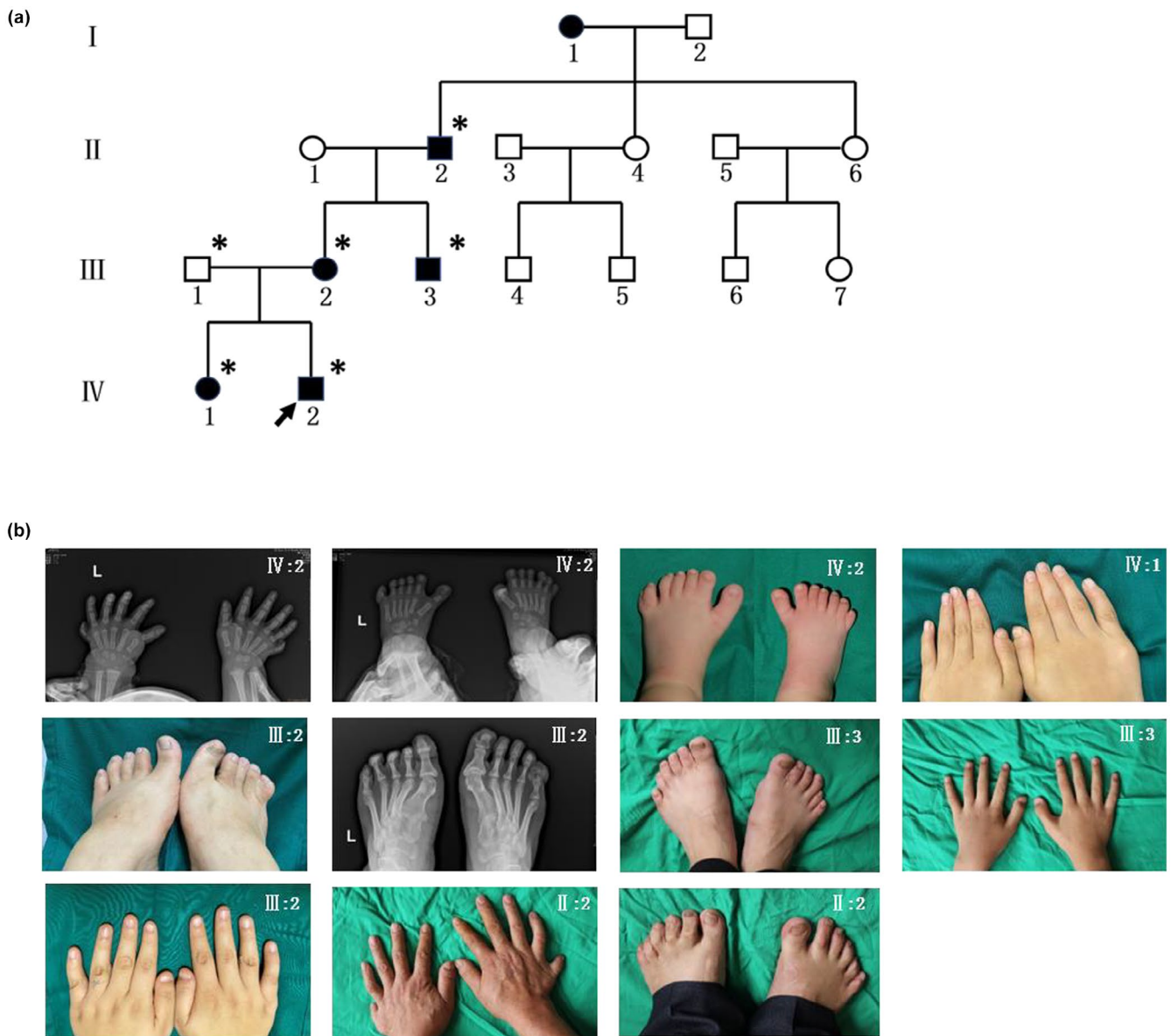


FIGURE 1 Clinical features of the affected members in Family 1. (a) Pedigree structure of a four-generation Chinese family with complex digital anomalies. Squares and circles denote males and females. Filled shapes indicate affected members. The arrow denotes the proband. Members marked with * are the participants in this study. (b) Clinical features of the proband (IV:2) and affected individuals (IV:1/III:2/III:3/II:2) are listed in Table 1

TABLE 1 The symptoms of digits abnormalities in five affects members of Family 1

Family and patient's ID	Lower limb			Upper limb			Clinical diagnosis
	Preaxial polydactyly	Syndactyly	Postaxial polydactyly	Preaxial polydactyly	Syndactyly	Postaxial polydactyly	
IV:2	Bil	Bil (2–3,6–7)	Bil	—	—	Bil	SPD 1
IV:1	—	—	—	—	—	Bil [†]	SPD 1
III:2	R	R (4–6)	R	—	—	Bil [†]	SPD 1
III:3	—	Bil (1–3) ^a	Bil ^a	—	—	Bil [†]	SPD 1
II:2	—	—	Bil	—	—	Bil	SPD 1

Abbreviations: Bil, bilateral; R, right; SPD, synpolydactyly.

^aMalformations were surgically corrected.

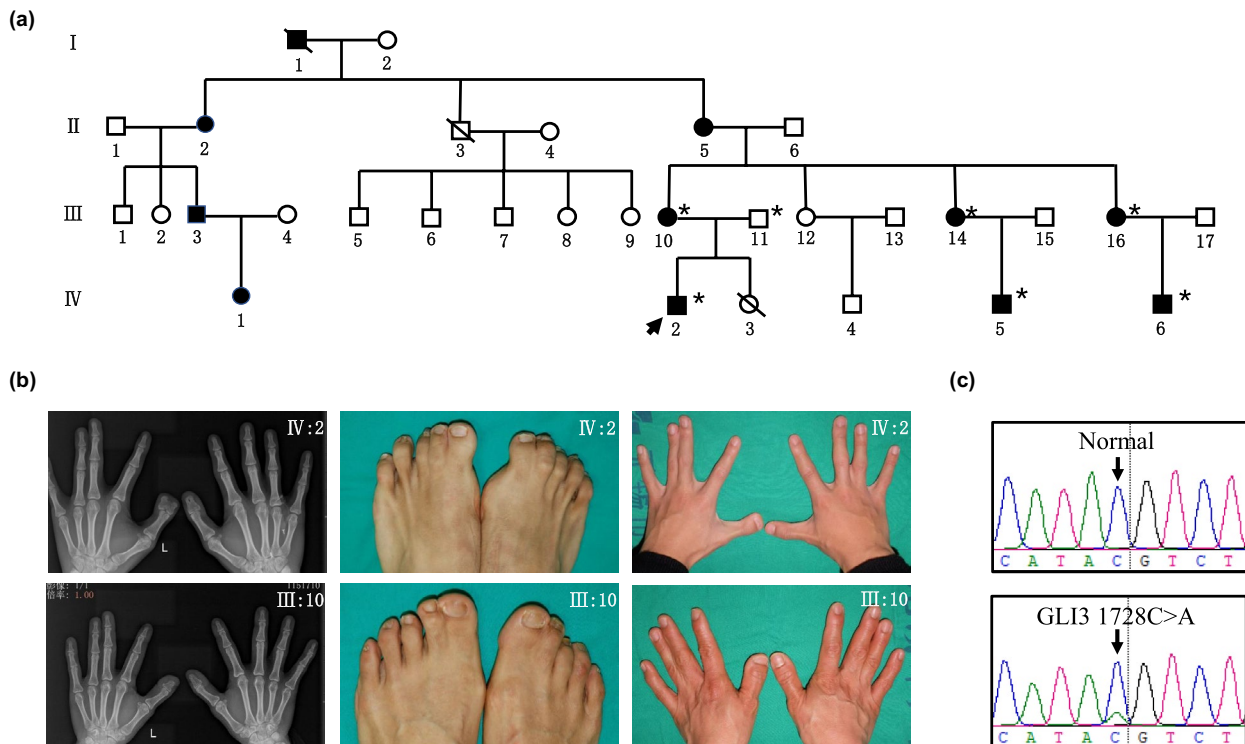


FIGURE 2 Clinical features of the affected members in Family 2. (a) Pedigree structure of a four-generation Chinese family with complex digital anomalies. Squares and circles denote males and females. Filled shapes indicate affected members. Individuals labeled with solidi are deceased. the arrow denotes the proband. Members marked with * are the participants in this study. (b) Clinical features of the proband (IV:2) and affected individuals (IV:5/IV:6/III:10/III:13/II:15) are listed in Table 2. (c) Sanger sequencing electropherograms of the variant (c.1728C>a, pY576X) identified in the *GLI3* gene

3.2 | Identification of point variants in the *GLI3*

To identify variants that predispose to syndactyly and polydactyly, whole-exome sequencing was initially performed on affected individuals and healthy members of these two pedigrees. In Family 1, IV:1, IV:2, III:1, III:2, III:3, II:1, and II:2 were subjected to whole-exome sequencing. In Family 2, IV:2, III:10, and III:11 were subjected to whole-exome sequencing. As previously reported (Zhou

et al., 2019), we annotated and filtered variants and kept variants that were novel in dbSNP. Polyphen-2, Mutation Taster, and Genomic Evolutionary Rate Profiling (GERP) were then used to predict the potential functional effects of these mutations.

In Family 1, we identified 10 candidate single nucleotide variations (SNVs), in which c.C2374T (Refseq NM_000168) in the *GLI3* (MIM:165240) has been reported to be associated with syndactyly and polydactyly (Table 4) (Furniss et al., 2007). In Family 2, we identified

TABLE 2 The symptoms of digits abnormalities in six affects members of Family 2

Family and patient's ID	Lower limb			Upper limb			Clinical diagnosis
	Preaxial polydactyly	Syndactyly	Postaxial polydactyly	Preaxial polydactyly	Syndactyly	Postaxial polydactyly	
IV:2	Bil	Bil (1–3)	—	Bil	Bil (3–4)	—	SPD 3
IV:5	Bil	Bil (1–2)	—	—	—	—	SPD 3
IV:6	—	L (1–2), R (1–3)	—	Bil	Bil (3–4)	—	SPD 3
III:10	—	Bil (1–2)	—	—	L (3–4)	—	SPD 3
III:14	L	—	—	—	L (3–4)	—	SPD 3
III:16	Bil	—	—	—	—	—	SPD 3

Abbreviations: Bil, bilateral; R, right; L, left; SPD, synpolydactyly.

Sample	IV:2	III:11	III:10
Total reads	89,485,646	107,931,572	96,863,472
Duplicate	21.38%	24.54%	22.22%
Mapped	99.98%	99.98%	99.98%
On target rate	80.91%	83.57%	83.18%
On target mean coverage 1X	112.65	134.82	123.73
On target mean mapping quality	57.90	57.82	57.84
Fraction of target covered with at least 1x	99.12%	99.46%	99.39%
Fraction of target covered with at least 10x	94.00%	95.11%	94.60%
Fraction of target covered with at least 50x	71.74%	76.04%	74.06%

TABLE 3 Depth and coverage of whole-exome sequencing in Family 2

TABLE 4 Detailed information for GLI3 c.C2374T after annotation

cDNA	GLI3 c.C2374T
Amino acid change	GLI3 p.R792X
In dbSNP or not	YES
Function GVS	Nonsense mutation
ConsScore GERP	3.7
phastCons20way_mammalian	0.956
phyloP20way_mammalian	0.079
Mutation Taster	1(Disease-causing-automatic)

Note: GenBank reference sequence and version number: NC_000007.13.

three candidate SNVs. Then by using Sanger sequencing, we excluded the SNV on *WDR34* and *FREM2*, because *GLI3* c.C1728A (Refseq NM_000168) turned out to be the only one that cosegregated with disease phenotypes in this family (Table 5). The location of *GLI3* p.R792X and p.Y576X were presented (Figure 3a). The *GLI3* p.Y576X was located in the ZNF domain and the

TABLE 5 Detailed information for GLI3 c.C1728A after annotation

cDNA	GLI3 c.C1728A
Amino acid change	GLI3 p.Y576X
In dbSNP or not	NONE
Function GVS	Nonsense mutation
ConsScore GERP	−3.75
phastCons20way_mammalian	0.974
phyloP20way_mammalian	−0.738
Mutation Taster	1(Disease-causing-automatic)

Note: GenBank reference sequence and version number: NC_000007.13.

GLI3 p.R792X was located outside the ZNF domain. According to American College of Medical Genetics and Genomics (ACMG) standards and guidelines, the new variant in Family 2 was classified as pathogenic. According to the Mutation Taster, the *GLI3* p.R792X and p.Y576X locus both showed conservation between species (Figure 3b).

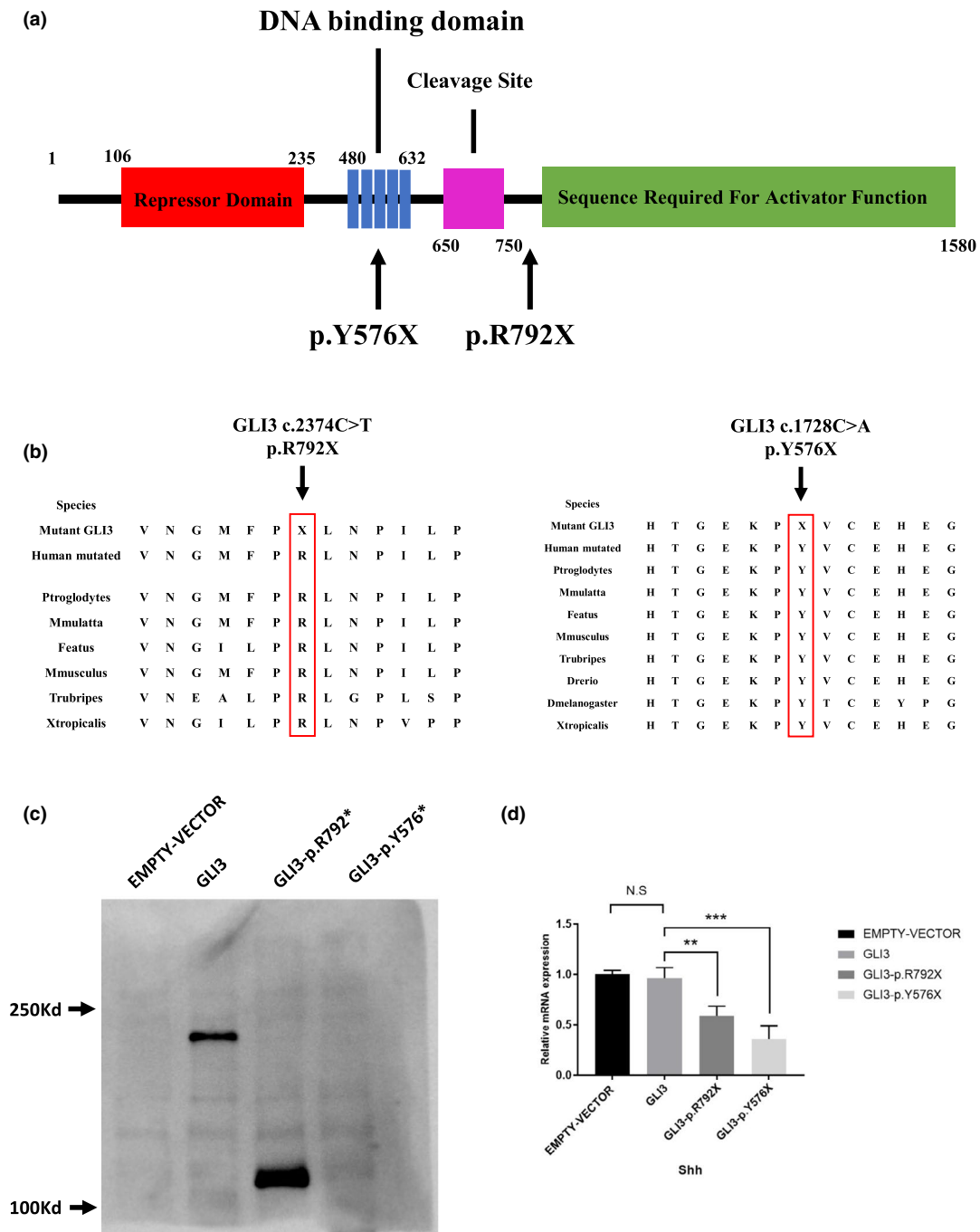


FIGURE 3 GLI3 variants led to truncated or degraded of GLI3 protein and decreased Shh expression. (a) The location of p.Y576X and p.R792X variants within GLI3 protein. (b) Comparison of the partial amino acid sequence of human GLI3 with other species. The boxed amino acid indicates the conserved residue across different species. (c) Western blotting analysis of the ectopic expression of GLI3 wild-type and mutant plasmids in HEK293T cells. (d) qPCR analysis of the Shh expression of GLI3 wild-type and mutant plasmids in limb bud cells ($n = 3$) * $p < .05$ (Student's t -test). N.S., not significant. Data are presented as mean \pm SD

3.3 | Functional studies on the GLI3 c.C2374T and c.C1728A variants

To further explore the functional consequences of these variants, c.2374C>T and c.1728C>A mutant plasmids and GLI3 wild-type plasmid were constructed. To validate these two nonsense mutations, we transfected these

plasmids into HEK293T cells separately. Compared with the wild-type GLI3, the Western blotting analysis showed that the GLI3 p.R792X protein was shorter (Figure 3c), whereas the GLI3 p.Y576X was undetectable, maybe due to the degradation of GLI3 p.Y576X protein (Figure 3c). To investigate whether these two GLI3 nonsense variants affected SHH signaling pathway, we then transfected the

wild-type and mutant plasmids into mice limb bud cells separately. The qPCR analysis showed that c.C2374T and c.C1728A variants in *GLI3* led to decreased Shh expression compared with the wild-type *GLI3* (Figure 3d). In conclusion, these two *GLI3* nonsense mutations may result in syndactyly and polydactyly by affecting the SHH signaling.

4 | DISCUSSION

In the presence of SHH signaling, *GLI3* is maintained as *GLI3*-FL form which induces its downstream target genes, such as *Patched1* (*Ptch1*). However, in the absence of SHH signaling, *GLI3* is either phosphorylated, ubiquitinated, and then partially degraded. The short form of *GLI3* is *GLI3*-R, which represses the transcription of its downstream target genes (Xiang et al., 2020). The mutations in *GLI3* are closely related to congenital limb malformations such as GCPS and PHS. Individuals suffering from GCPS are characterized by preaxial polydactyly of the feet, postaxial polysyndactyly of the hands, and macrocephaly. In GCPS, mutations in *GLI3* include missense mutations, splicing mutations, deletions, insertions, and translocations. These mutations can occur throughout the *GLI3* protein and disrupt the balance between *GLI3*-R and *GLI3*-FL, resulting in the lack of negative regulation of SHH signaling (Johnston et al., 2010; Abdullah Yousaf et al., 2019). PHS is clinically identified by mesoaxial polydactyly and hypothalamic hamartoma. In PHS, mutations in *GLI3* include frameshift and nonsense mutations, which lead to a truncated version of *GLI3* (691 AA long). This truncated *GLI3* showed inhibitory functions similar to *GLI3*-R in the context of SHH signaling (Böse et al., 2002; Kang et al., 1997). These studies demonstrate the importance of *GLI3* in limb development.

Shh is expressed at the posterior margin of the limb buds in vertebrates, specifying an anteroposterior pattern in developing limbs by stimulating the proliferation of mesenchyme and regulating the anteroposterior length of the apical ectodermal ridge. As we previously reported, ectopic anterior expression of SHH in the hindlimbs led to preaxial polydactyly in ZRS g.101779T>A homozygous mice models (Xu et al., 2020). Yoshiyuki et al. demonstrated that a severe lack of SHH signaling led to the polydactyly, syndactyly, and brachydactyly in homozygote hereditary multiple malformation mutant (*hmm*^{-/-}) mouse embryos. In the *hmm*^{-/-} limb bud, Shh was restricted to a more proximal region of the forelimb bud than in the *hmm*^{+/-} limb bud. Besides *Gli1*, *Ptch1*, *Ptch2*, and *Bmp2* which are known to be downstream target genes of SHH signaling showed decreased expression

(Matsubara et al., 2016). It is frequently described that altered Shh signaling is involved in congenital digit malformations under clinical conditions. Under the delicate regulation between *GLI3* and SHH signaling, the limb bud revolves into normal digits.

In our study, we transfected *GLI3* c.2374C > T and c.1728C > A mutant plasmids into HEK293T cells. The *GLI3* c.C2374T variant led to truncated *GLI3* protein, and the *GLI3* c.C1728A variant led to degraded *GLI3* protein. We assumed that this kind of truncated or degraded *GLI3* protein may affect the SHH signaling, resulting in polydactyly and syndactyly phenotype in these two families. Then we transfected the mutant plasmids into the mouse limb bud cells to detect the changes in Shh expression. Surprisingly, we found that mutant plasmids led to decreased Shh expression. The dysfunction of SHH signaling was responsible for the polydactyly and syndactyly in these two families.

5 | CONCLUSION

We demonstrated that the novel *GLI3* variant (c.1728C>A) and known *GLI3* variant (c.2374C>T) contributed to the malformations in two four-generation pedigrees with polydactyly and syndactyly. The *GLI3* c.C1728A variant led to truncated *GLI3* protein and the *GLI3* c.2374C>T variant led to degraded *GLI3* protein. Both the mutant plasmids led to decreased Shh expression, which resulted in limb malformation.

ACKNOWLEDGMENTS

The HEK293T cells were generally gifted by Prof. Dongsheng Huang from the Department of Orthopedics, Sun Yat-sen Memorial Hospital of Sun Yat-sen University.

CONFLICT OF INTEREST

The authors declare that they have no conflict of interest.

AUTHORS' CONTRIBUTIONS

RYJ and ZTF conceived the idea and provided scientific support and professional guidance; SXF and ZS designed the project, conducted experiments, analyzed the data, performed statistical analyses, and wrote the manuscript; ZX revised the manuscript.

ETHICAL COMPLIANCE

The study was approved by the ethics committee of the Wuxi Ninth People's Hospital Affiliated to Soochow University. All experimental protocols were approved by the ethics committee of the Wuxi Ninth People's Hospital Affiliated to Soochow University and were carried out in accordance with the approved guidelines. Each individual

in these two families undergoing the genetic test was adequately informed regarding the benefits and risks of the test and signed the consent forms.

DATA AVAILABILITY STATEMENT

The data that support the findings of this study are available from the corresponding author upon reasonable request.

ORCID

Yongjun Rui  <https://orcid.org/0000-0003-1742-0186>

REFERENCES

- Abdullah Yousaf, M., Azeem, Z., Bilal, M., Liaqat, K., Hussain, S., Ahmad, F., Ghous, T., Ullah, A., & Ahmad, W. (2019). Variants in GLI3 cause Greig cephalopolysyndactyly syndrome. *Genetic Testing and Molecular Biomarkers*, 23(10), 744–750. <https://doi.org/10.1089/gtmb.2019.0071>
- Al-Qattan, M. M., Shamseldin, H. E., Salih, M. A., & Alkuraya, F. S. (2017). GLI3-related polydactyly: A review. *Clinical Genetics*, 92(5), 457–466. <https://doi.org/10.1111/cge.12952>
- Anderson, E., Peluso, S., Lettice, L. A., & Hill, R. E. (2012). Human limb abnormalities caused by disruption of hedgehog signaling. *Trends in Genetics*, 28(8), 364–373. <https://doi.org/10.1016/j.tig.2012.03.012>
- Biesecker, L. G. (2008). The Greig cephalopolysyndactyly syndrome. *Orphanet Journal of Rare Diseases*, 3(10), 1–6. <https://doi.org/10.1186/1750-1172-3-10>
- Böse, J., Grotewold, L., & Rütther, U. (2002). Pallister-Hall syndrome phenotype in mice mutant for Gli3. *Human Molecular Genetics*, 11(9), 1129–1135. <https://doi.org/10.1093/hmg/11.9.1129>
- Furniss, D., Critchley, P., Giele, H., & Wilkie, A. O. (2007). Nonsense-mediated decay and the molecular pathogenesis of mutations in SALL1 and GLI3. *American Journal of Medical Genetics. Part A*, 143a(24), 3150–3160. <https://doi.org/10.1002/ajmg.a.32097>
- Gao, W., Chen, C., Zhou, T., Yang, S., Gao, B., Zhou, H., Lian, C., Wu, Z., Qiu, X., Yang, X., & Su, P. (2017). Rare coding variants in MAPK7 predispose to adolescent idiopathic scoliosis. *Human Mutation*, 38(11), 1500–1510. <https://doi.org/10.1002/humu.23296>
- Hall, J. G. (2014). Pallister-Hall syndrome has gone the way of modern medical genetics. *American Journal of Medical Genetics. Part C, Seminars in Medical Genetics*, 166c(4), 414–418. <https://doi.org/10.1002/ajmg.c.31419>
- Johnston, J. J., Olivos-Glander, I., Killoran, C., Elson, E., Turner, J. T., Peters, K. F., ... Biesecker, L. G. (2005). Molecular and clinical analyses of Greig cephalopolysyndactyly and Pallister-Hall syndromes: Robust phenotype prediction from the type and position of GLI3 mutations. *American Journal of Human Genetics*, 76(4), 609–622. <https://doi.org/10.1086/429346>
- Johnston, J. J., Sapp, J. C., Turner, J. T., Amor, D., Aftimos, S., Aleck, K. A., Bocian, M., Bodurtha, J. N., Cox, G. F., Curry, C. J., & Day, R. (2010). Molecular analysis expands the spectrum of phenotypes associated with GLI3 mutations. *Human Mutation*, 31(10), 1142–1154. <https://doi.org/10.1002/humu.21328>
- Jordan, D., Hindocha, S., Dhital, M., Saleh, M., & Khan, W. (2012). The epidemiology, genetics and future management of syndactyly. *The Open Orthopaedics Journal*, 6, 14–27. <https://doi.org/10.2174/1874325001206010014>
- Kang, S., Graham, J. M., Jr., Olney, A. H., & Biesecker, L. G. (1997). GLI3 frameshift mutations cause autosomal dominant Pallister-Hall syndrome. *Nature Genetics*, 15(3), 266–268. <https://doi.org/10.1038/ng0397-266>
- Matissek, S. J., & Elsawa, S. F. (2020). GLI3: A mediator of genetic diseases, development and cancer. *Cell Communication and Signaling: CCS*, 18(1), 1–20. <https://doi.org/10.1186/s12964-020-00540-x>
- Matsubara, Y., Nakano, M., Kawamura, K., Tsudzuki, M., Funahashi, J. I., Agata, K., Matsuda, Y., Kuroiwa, A., & Suzuki, T. (2016). Inactivation of sonic hedgehog signaling and polydactyly in limbs of hereditary multiple malformation, a novel type of Talpid mutant. *Frontiers in Cell and Development Biology*, 4(149), 1–13. <https://doi.org/10.3389/fcell.2016.00149>
- Petit, F., Sears, K. E., & Ahituv, N. (2017). Limb development: A paradigm of gene regulation. *Nature Reviews. Genetics*, 18(4), 245–258. <https://doi.org/10.1038/nrg.2016.167>
- Villavicencio, E. H., Walterhouse, D. O., & Iannaccone, P. M. (2000). The sonic hedgehog-patched-gli pathway in human development and disease. *American Journal of Human Genetics*, 67(5), 1047–1054. [https://doi.org/10.1016/s0002-9297\(07\)62934-6](https://doi.org/10.1016/s0002-9297(07)62934-6)
- Vortkamp, A., Gessler, M., & Grzeschik, K. H. (1991). GLI3 zinc-finger gene interrupted by translocations in Greig syndrome families. *Nature*, 352(6335), 539–540. <https://doi.org/10.1038/352539a0>
- Xiang, Y., Li, X., Zhan, Z., Feng, J., Cai, H., Li, Y., Fu, Q., Xu, Y., Jiang, H., & Zhang, X. (2020). A novel nonsense GLI3 variant is associated with polydactyly and syndactyly in a family by blocking the sonic hedgehog signaling pathway. *Frontiers in Genetics*, 11(542004), 1–10. <https://doi.org/10.3389/fgene.2020.542004>
- Xu, C., Yang, X., Zhou, H., Li, Y., Xing, C., Zhou, T., Zhong, D., Lian, C., Yan, M., Chen, T., Liao, Z., & Su, P. (2020). A novel ZRS variant causes preaxial polydactyly type I by increased sonic hedgehog expression in the developing limb bud. *Genetics in Medicine*, 22(1), 189–198. <https://doi.org/10.1038/s41436-019-0626-7>
- Zhou, H., Lian, C., Wang, T., Yang, X., Xu, C., Su, D., Zheng, S., Huang, X., Liao, Z., Zhou, T., Qiu, X., & Su, P. (2019). MET mutation causes muscular dysplasia and arthrogryposis. *EMBO Molecular Medicine*, 11(3), 1–9. <https://doi.org/10.15252/emmm.201809709>

How to cite this article: Shen, X., Zhang, S., Zhang, X., Zhou, T., & Rui, Y. (2022). Two nonsense GLI3 variants are associated with polydactyly and syndactyly in two families by affecting the sonic hedgehog signaling pathway. *Molecular Genetics & Genomic Medicine*, 10, e1895. <https://doi.org/10.1002/mgg3.1895>